Journal of Alloys and Compounds 567 (2013) 59–64

Contents lists available at SciVerse ScienceDirect

Journal of Alloys and Compounds

journal homepage: www.elsevier.com/locate/jalcom

Transformation of austenite during isothermal annealing at 600–900 °C for heat-resistant stainless steel

Ladislav Kosec [a], Štefan Šavli [b], Stjepan Kožuh [c], Tamara Holjevac Grgurić [c], Aleš Nagode [a], Gorazd Kosec [d], Goran Dražić [e], Mirko Gojić [c,*]

[a] University of Ljubljana, Faculty of Natural Sciences and Engineering, Aškerčeva 12, 1000 Ljubljana, Slovenia
[b] Iskra avtoelektrika, Polje 15, 5290 Sempeter pri Gorici, Slovenia
[c] University of Zagreb, Faculty of Metallurgy, Aleja narodnih heroja 3, 44103 Sisak, Croatia
[d] Acroni d.o.o., Cesta Borisa Kidrica 44, 4270 Jesenice, Slovenia
[e] Jožef Stefan Institute, Jamova cesta 39, 1000 Ljubljana, Slovenia

ARTICLE INFO

Article history:
Received 26 October 2012
Received in revised form 19 February 2013
Accepted 2 March 2013
Available online 21 March 2013

Keywords:
High-temperature alloys
Precipitation
Microstructure
Scanning electron microscopy
Thermal analysis
Transmission electron microscopy

ABSTRACT

In this work, the results of the transformation kinetics of austenite heat-resistant stainless steel (AISI 310S) with 2.27 wt.% silicon were presented. The results of microstructural and fractography analysis, as well as the results of hardness after the isothermal heat treatment of the steel in the temperature range from 600 to 900 °C at different annealing times (from 1 to 956 h) are shown. It was found that the microstructure of steel after isothermal annealing consisted of austenite, carbide ($M_{23}C_6$) and σ-phase. The number of σ-phase precipitates increases with higher annealing times. In longer annealed steel samples the significant coarsening of precipitates was observed, as well as a large amount of σ-phase particles in the form of a chain and a network of plates. Precipitates were both observed at grain boundaries and within austenite grains. σ-phase precipitation involves two mechanisms: transformation $\gamma \rightarrow Cr_{23}C_6 \rightarrow \sigma$ and transformation $\gamma \rightarrow \alpha' \rightarrow \sigma$. The hardness began to increase after 48 h of annealing at a temperature of 600 °C, while in the temperature range of 700–900 °C the hardness increased with annealing times higher than 8 h. The slope of hardness curve is caused by microstructural changes. The fracture surface mode was intercrystalline brittle. Relatively large dimples can be related to large particles of precipitates which occurred after long annealing times.

1. Introduction

Stainless steels offer a combination of good mechanical properties and good corrosion resistance. Today, they are well established in many applications. Among others, heat-resistant austenite steels are very interesting due to applications for high-temperature conditions. These steels have better strength and oxidation resistance at high temperatures than low-alloyed steels and they are less expensive than Ni-base alloys. It is known that heat-resistant austenitic stainless steels have a tendency to form different phases [1,2]. The microstructure of heat-resistant austenitic steels after isothermal annealing is quite complex, especially in the temperature range from 600 to 900 °C. Heat-resistant steel can contain numerous precipitates such as carbides and intermetallic phases [3–5]. Zhang et al. [6] showed that $M_{23}C_6$-type carbides precipitated first along the grain boundaries and then inside the grains in the case of S30432 heat-resistant steel during aging at 650 °C. Carbide precipitates at grain boundaries provide preferential sites for cavity nucleation owing to the stress concentration produced during the fatigue cycle.

The most frequently found intermetallic phase in austenitic steels is the hard and brittle σ-phase. If the σ-phase is present in significant amounts it has the effect of reducing the ductility (i.e. the elongation and reduction of an area at fracture) and toughness of the steel. The σ-phase is also detrimental to crevice and pitting corrosion resistance and this negative influence is attributed to the depletion of chromium and molybdenum at the grain boundaries [7,8]. The precipitation of carbides and the σ-phase promote the sensitivity of steel, i.e. they increase the susceptibility of the steel to intergranular corrosion.

Although the precipitation mechanism of the phases has been investigated extensively, important discrepancies remain [1–9]. Also, the kinetics of its formation is rather obscure. For AISI 321 stabilized austenitic stainless steel aged at 600 and 700 °C the beginning of σ-phase precipitation is detected for 2 h. Park et al. [10] suggested that the rapid precipitation of the σ-phase in AISI 304 stainless steel is related to the transformation of austenite to δ-ferrite during friction stir welding. The formation of the σ-phase can occur in austenite/austenite, δ-ferrite/austenite interface,

* Corresponding author. Tel.: +385 44 533 381; fax: +385 44 533 378.
E-mail address: gojic@simet.hr (M. Gojić).

0925-8388/$ - see front matter © 2013 Elsevier B.V. All rights reserved.
http://dx.doi.org/10.1016/j.jallcom.2013.03.102

δ-ferrite/δ-ferrite, etc. It is reported that the chemical composition of the σ-phase shows considerable variation. The composition of the σ-phase in austenitic stainless steels can differ [11,12]. In order to better understand its behavior, the results of the austenite transformation of heat-resistant stainless steel with 2.27% silicon (wt.%) after isothermal annealing in the temperature range from 600 to 900 °C at different annealing times (from 1 to 956 h) were presented.

2. Experimental

Heat-resistant stainless steel with 2.27 wt.% silicon was tested (Table 1). Investigated steel samples were received in the form of pipes. Prior to solution heat treatment, the samples were cut to the dimensions 120 × 25 × 5 mm, and then heated in an electro-arc furnace with air atmosphere. The solution heat treatment was performed at 1100 °C/15 min followed by quenching in water (15 °C). After quenching, samples were cut to the dimensions 25 × 12 × 5 mm and isothermally annealed in the temperature range from 600 to 900 °C. Samples were annealed at times from 5 min to 956 h in an electro-arc furnace with air atmosphere. Subsequently, the samples were cooled by air. After annealing the microhardness, a test was carried out using the Vickers method (HV0.3). The thermodynamic calculation of equilibrium phases using the ThermoCalc TCW5 program was performed. The microstructural analysis was carried out by scanning electron microscopy (SEM) and transmission electron microscopy (TEM), respectively. The fractographic analysis was performed by SEM. The samples for the microstructural analysis were subsequently grounded (paper gradations 220–1200), mechanically polished with diamond paste (3 μm) and oxide polish. Afterwards, the samples were electrolitically etched in 10% oxalic acid in an H_2O solution at 20 °C. Etching was carried out very quickly (3 s) at 2.5 V at a current density of 1.69 mA/cm^2. The fractographic analysis was carried out with the Jeol JSM-5610, which was equipped with the EDXS system. TEM samples were prepared by mechanical thinning, dimpling and ion milling using 3.8 keV argon ions. Samples were characterized by the Jeol J-2100 200 kV transmission electron microscope, which was equipped with a Si(Li) energy-dispersive X-ray spectrometer (EDXS). For phase identification, selected area electron diffraction (SAED) and micro-diffraction were used.

3. Results and discussion

In order to estimate the fraction of each phase and the temperature range stability, the Thermocalc program was used for the exact composition of the steel (Table 1). Fig. 1 shows the composition of phases in the steel as a function of temperature. The Thermocalc calculation indicates that austenite, $M_{23}C_6$ and the σ-phase are presented. In equilibrium conditions, the content of the σ-phase decreases from 600 to 900 °C, while the $M_{23}C_6$ content is very low and almost constant. Figs. 2 and 3 show SEM micrographs of the steel after annealing at different temperatures. As can be seen from Figs. 2 and 3, the transformation of austenite is accompanied by the formation of σ-phase particles along austenitic grain boundaries due to energetically favorable heterogeneous nucleation. It is also apparent that the amount of σ-phase increases with increasing exposure time.

In the steel sample annealed at 700 °C for 1 h, the existence of very small (1–2.8 μm) and sporadically distributed particles of the precipitated σ-phase can be seen (Fig. 2a). By increasing the annealing time, the number of σ-phase particles increases and becomes coarser (Fig. 2a–d). The particle size of the σ-phase can occur in the interval from 3.8 to 10.6 μm at 956 h. Similar behavior of the σ-phase, with respect to the influence of annealing time on size and morphology, was observed after annealing at 800 °C (Fig. 3). Large particles coexist with other smaller intergranular and transgranular particles. In steel samples annealed at longer times, the coarsening of precipitates is significant and a large

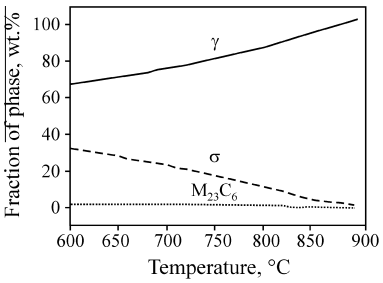

Fig. 1. Phase fraction in AISI 310S steel in equilibrium conditions.

amount of σ-phase particles in the form of the chain and network of plates is observed. In this case, the precipitates were observed at grain boundaries but also within the austenite grains. Chromium atoms gradually diffuse up from the austenite matrix to the austenite/austenite grain boundary during annealing to produce an equilibrium concentration. When the chromium and iron at the austenite/austenite grain boundary achieve a critical value, the σ-phase can be formed.

In this work, it was found that the formation kinetics of the σ-phase is faster than for AISI 347 or AISI 321 steels [13]. Also, the particles of the σ-phase at the austenitic grain boundary coarsen and growth with time. This is in accordance with the results of Tavares et al. [14] who found that σ-phase precipitation nucleated at grain boundaries and became more intensive with the increasing of time and the temperature of AISI 310S steel exposed at 600–800 °C for up to 210 h. By increasing the annealing time, the formation of the σ-phase in the form of the plate expanded into austenitic grains. After annealing at 700 °C for 956 h, the austenite matrix was completely covered with the sigma phase (Figs. 2d and 3d). Zones near the grain boundaries are depleted due to the diffusion of elements. The concentration of chromium in the sigma phase is increased, while concentrations of iron and nickel are decreased (Table 2).

The opposite investigations of the nucleation of the σ-phase can be found in literature. Schwind et al. [15] investigated σ-phase precipitation in austenite stainless steel and found that the σ-phase requires the redistribution of alloying elements (especially chromium) by substitution diffusion in the matrix. Diffusion in solids is a very slow process, thus small amounts of the σ-phase were detected at lower annealing temperatures (600 and 700 °C) and lower annealing times (1 and 24 h). Further, the redistribution of chromium along grain boundaries is much more effective than in the grains and precipitation first started at grain boundaries. Coreño-Alonso et al. [16] investigated similar steel (23–27% Cr, 19–22% Ni, 1.5% Mn, 1.75% Si) and concluded that the direct transformation of austenite to the σ-phase can occur after exposing the steel to higher temperatures (760–870 °C). However, the direct decomposition of austenite to the σ-phase is difficult because it requires a long period of time due to the redistribution of alloying elements. Usually, the σ-phase can occur by the transformation of carbide ($M_{23}C_6$) or ferrite. Kington and Noble [17] reported that the isothermal formation of ferrite from austenite in 310 steel may occur. This ferrite (α′) begins to form between 800 and 900 °C. They also reported that the α′-phase is not stable in 310 steel at high temperatures, so it must nucleate metastably. Its composition is changed as it grows into the surrounding unstable austenite. It is

Table 1
Chemical composition of heat-resistant stainless steel (wt.%).

C	Si	Mn	P	S	Cr	Mo	Ni	Cu	Ti	Al	Co	Nb
0.059	2.27	1.54	0.029	0.014	23.38	0.18	20.13	0.23	0.015	0.065	0.09	0.007